Journal of Hazardous Materials 186 (2011) 690–698

Contents lists available at ScienceDirect

Journal of Hazardous Materials

journal homepage: www.elsevier.com/locate/jhazmat

The influence of ferric iron in calcined nano-Mg/Al hydrotalcite on adsorption of Cr (VI) from aqueous solution

Lili Xiao, Wei Ma*, Mei Han, Zihong Cheng

College of Chemistry, Dalian University of Technology, Dalian, Liaoning 116023, PR China

ARTICLE INFO

Article history:
Received 5 April 2010
Received in revised form 23 October 2010
Accepted 12 November 2010
Available online 20 November 2010

Keywords:
Ferric iron
Structure memory
Calcined hydrotalcite
Chromium (VI)
Adsorption

ABSTRACT

The influence of ferric iron in calcined nano-Mg/Al hydrotalcite on removal of Cr (VI) from aqueous solution was studied from aspects of structure characteristics, adsorption properties and mechanism discussions. The calcined hydrotalcites (CH–Mg/Al and CH–Mg/Al/Fe) were obtained by thermal decomposition of their corresponding precursors and characterized by XRD, TEM, pH_{PZC} and FTIR. The adsorption properties were studied as a function of pH, initial Cr (VI) concentration and contact time. The results showed that the nature of adsorption is endothermic and spontaneous for both CH–Mg/Al and CH–Mg/Al/Fe, but the thermodynamic parameter value changes revealed the addition of Fe^{3+} is disadvantage to adsorption process and the theoretical saturated adsorption capacity decreased by approximately 10.2 mg/g at tested temperatures. The removal mechanism involved not only intercalation but adsorption on external surface of the layers and interlayer anion exchange for both CH–Mg/Al and CH–Mg/Al/Fe. Furthermore, the results also indicated that intercalation accounts for a large proportion during removal process whatever for CH–Mg/Al, or for CH–Mg/Al/Fe. Additionally, the replacement of Al^{3+} by Fe^{3+} in CH–Mg/Al led to the interlayer anion exchange more difficult. On the basis of the results, it is concluded that the existence of ferric iron in calcined Mg/Al hydrotalcite is unfavorable to removal of Cr (VI) from aqueous solution.

1. Introduction

Hydrotalcites are layered metal double hydroxides with the general formula $[M_{1-x}^{2+}M_x^{3+}(OH)_2](A^{n-})_{x/n}\cdot mH_2O]$, where M^{2+} is the divalent cation (Mg^{2+}, Zn^{2+}, Ni^{2+} etc.); M^{3+} is the trivalent cation (Al^{3+}, Fe^{3+}, Cr^{3+} etc.); A^{n-} is the anion (CO_3^{2-}, NO_3^-, Cl^- etc.) and x is defined as the $M^{3+}/M^{2+}+M^{3+}$ ratio with various values between 0.2 and 0.33. These materials consist of positively charged brucite layers, which are compensated by anions and water molecules in the interlayer region [1,2]. The large interlayer space and significant number of exchangeable anions make hydrotalcites attractive for applications as adsorbents and ion-exchangers [3]. Hydrotalcites uptake anions from aqueous solution via three mechanisms: (i) adsorption on external surface; (ii) intercalation by anion exchange; (iii) intercalation by reconstruction of calcined products. The last phenomenon, known as "structure memory effect", takes place when hydrotalcites are calcined to eliminate most of the interlayer anions followed by rehydration; anions are incorporated and the calcined hydrotalcites "recover" their original layered structure [4]. Reconstruction occurs only in a given temperature range where the thermal decomposition is performed. The calcined temperature must be high enough to eliminate most of the anions of the interlayer. However, if the calcined temperature is too high such as higher than 600 °C, stable $M^{III}M^{II}{}_2O_4$ spinel and $M^{II}O$ phases are formed and hydrotalcites can not be reconstructed [5]. Recently, the high anion exchange capacity and "memory effect" make hydrotalcites and their calcined products as the promising adsorption materials for anions removal, such as the removal of chromium (VI) [6,7].

Cr (VI) is highly mobile and mutagenic as a priority list of pollutants, which not only damages plant and animal tissues but also gives rise to varieties of diseases in humans even in small quantities [8]. In recent years, the release of Cr (VI) into water system has become more and more seriously with the development of some industries such as paint, leather tanning, pigment manufacturing in China [9]. Therefore, it is imperative to remove Cr (VI) from aqueous solution.

The methods used to remove Cr (VI) from the wastewaters include membrane filtration, chemical precipitation, solvent extraction, adsorption, etc. [10,11]. Among these, adsorption as an effective physicochemical treatment process for removing heavy metal ions with lower concentration has come to the forefront [12]. A variety of materials such as carbon slurry [13], the modified chitosan [14], natural wood [15], activated alumina and activated charcoal [16], calcined magnesium aluminum hydrotalcite [17], aluminum magnesium mixed hydroxide [18] and amorphous alu-

* Corresponding author. Tel.: +86 411 8470 6303; fax: +86 411 8470 7416.
E-mail addresses: chmawv@yahoo.com, mawei@dlut.edu.cn (W. Ma).

0304-3894/$ – see front matter © 2010 Elsevier B.V. All rights reserved.
doi:10.1016/j.jhazmat.2010.11.052

minum oxide [8] have been used as adsorbents for removal of Cr (VI) from aqueous solution. Among these adsorbents, hydrotalcites and their calcined products have attracted increasing attention for their low cost, large adsorption capacity and their unique structure.

For these layered compounds, the most studied are the aluminum-based ones such as Mg/Al hydrotalcites and their calcined products [7,17]. However, the presence of Al may have a serious drawback when using these materials in drinking water treatment. Al exposure has been pointed out as a potential risk factor for either the development or the speeding up of the Alzheimer syndrome in human beings [19]. Considering this scenario, the search for a new material free from toxic metals such as Al, the iron based hydrotalcites appear as very promising candidates. At the same time, some researchers [20,21] have reported anions removal on calcined hydrotalcites with Fe-based hydrotalcites, but the removal efficiency is not ideal. Therefore, in order to reduce Al content, as well as try not to affect the adsorption capacity as much as possible, Al was substituted partly for ferric iron in our study. On the other hand, research about the influence of ferric iron in calcined Mg/Al hydrotalcite on removal of Cr (VI) from aqueous solution, especially on the relationship between structural changes and adsorption capacity during the adsorption process and the adsorption mechanism is limited. So the aim of this paper is to: (i) prepare and characterize two kinds of calcined hydrotalcites (CH–Mg/Al and CH–Mg/Al/Fe) by XRD, TEM and FTIR in order to investigate the effect of Fe^{3+} on CH–Mg/Al structure; (ii) discuss the influence of Fe^{3+} on adsorption properties; (iii) investigate the differences of nature and mechanism of adsorption on CH–Mg/Al and CH–Mg/Al/Fe.

2. Materials and methods

2.1. Adsorbents preparation

The calcined hydrotalcites (CH–Mg/Al and CH–Mg/Al/Fe) were obtained by thermal decomposition of their corresponding precursors. All chemical reagents used were AR grade, and all solutions were prepared with deionized water.

The precursors were synthesized by co-precipitation method. The nitrate solution (60 ml) with Mg/Al ratio equal to 3 or Mg/Al/Fe ratio equal to 3:0.8:0.2 was added drop-wise into the alkaline solution (80 ml) containing 2.0 mol/L NaOH and 0.5 mol/L Na_2CO_3 under vigorous stirring, respectively. The solution was stirred for 2 h continuously after the addition of nitrates. Then thick slurry was obtained with finial pH 10 ± 0.5, which was then heated for 24 h at 65 °C for ageing. Afterwards, the slurry was filtered and washed several times with deionized water until the effluent solution was neutral. Finally, the filter cake was dried at 80 °C for 24 h to obtain the precursors and then calcined for 4 h at 500 °C to obtain the calcined hydrotalcites signed as CH–Mg/Al and CH–Mg/Al/Fe, respectively. The precursor color of Mg/Al/Fe was pale and then turned to pale yellow with calcination.

2.2. Adsorbents characterization

Powder X-ray diffraction (XRD) analyses were carried out to identify the phase of Mg/Al and Mg/Al/Fe hydrotalcites, their calcined hydrotalcites, as also the solid samples after adsorption using a Shimadazu XRD-6000 X-ray diffractometer with Cu Kα radiation (λ = 1.54184 Å) at 35 kV and 25 mA. Scanning diffraction angle range is set as 5–70° at the speed of 0.06° s^{-1}.

The grain morphology and particle size of Mg/Al and Mg/Al/Fe hydrotalcites were observed by transmission electron microscopy (TEM) on a JEOL 2200FS at accelerating voltage of 200 kV and photomicrographs collected using a Hamamatsu CCD digital camera.

The pH at the point of zero charge (pH_{PZC}) of the calcined hydrotalcites was determined by different concentrations of NaCl with 0.1 mol/L and 0.05 mol/L as inert electrolytes. The initial pH was adjusted from 2.0 to 14.0 by addition of 0.1 mol/L HNO_3 or NaOH. The experiments were carried out in a thermostat shaker at 140 rpm and 35 °C for 2 h. Then the suspensions were filtered and the final pH values were measured. The pH_{PZC} was obtained through the plots pH_{final} versus $pH_{initial}$ [22].

Fourier transform infrared (FTIR) spectra of the calcined hydrotalcites and their solid samples after adsorption were recorded using KBr pellets over the 4000–400 cm^{-1} wavenumber range.

2.3. Adsorption experiments

A stock solution containing 1000 mg/L Cr (VI) was prepared by $K_2Cr_2O_7$. Batch experimental solutions were diluted for adsorption and analysis. The experiments were carried out in 150 ml stoppered conical flasks under constant shaking (140 rpm) in a thermostat shaker, and then centrifuged at 3500 rpm for 10 min before analyzed. The pH effect was studied within the range of 2.0–10.0 (adjusted with 0.1 mol/L HNO_3 or NaOH) with the initial Cr (VI) concentration of 50 mg/L and the contact time of 120 min at 308 K. Adsorption isotherms were conducted with initial Cr (VI) concentrations of 20, 50, 80, 110, 150 and 200 mg/L at 295–321 K in the initial pH 3.0 and the contact time of 120 min, and the effect of contact time was carried out at specific time intervals of 5, 10, 20, 30, 50, 70, 90 and 120 min with the initial Cr (VI) concentration of 50 mg/L and the initial pH 3.0 at 308 K. Above batch experiments were conducted under the same conditions of 50 ml chromium solution and adsorbent dose of 1.0 g/L. The colorimetric method with 1,5-diphenylcarbazide as the complexing agent was used for the determination of initial and finial Cr (VI) concentrations at λ = 540 nm. All experiments were carried out in duplicates and the deviation about the mean was less than five percent in all cases.

3. Results and discussion

The influence of ferric iron in CH–Mg/Al on removal of Cr (VI) was studied from the following aspects: structure characteristics, adsorption properties and the removal mechanism.

3.1. The structure characteristics of CH–Mg/Al and CH–Mg/Al/Fe

The XRD patterns of CH–Mg/Al and CH–Mg/Al/Fe and their precursors are shown in Fig. 1. The precursors of Mg/Al and Mg/Al/Fe (curves a and b) indicate that they both show sharp and symmetric peaks at (0 0 3) and (0 0 6), suggesting the characteristic of hydrotalcites with the layered double structure and a high degree of crystallinity [1]. Moreover, it shows that the characteristic peaks of Mg/Al precursor have not changed apart from the lower intensities and the smaller interlayer space by replacing with Fe^{3+}. The interlayer space calculated using (0 0 3) peak is 7.78 Å and 7.74 Å for Mg/Al and Mg/Al/Fe precursor, respectively. As we all know, the interlayer space depends on M^{2+}/M^{3+} molar ratio, metal ionic radius, the size of anion within the interlayer and the degree of hydration [23]. Therefore, the minor difference of d-spacing may be due to the larger ionic radius of ferric iron than aluminum ion.

When calcined Mg/Al and Mg/Al/Fe precursors, the characteristic peaks (0 0 3) and (0 0 6) of hydrotalcites disappeared regardless of CH–Mg/Al or CH–Mg/Al/Fe (curves c and d in Fig. 1), indicating that the hydrotalcite structure is seriously destroyed and there is disordering in the stacking of the layers.

TEM images of Mg/Al and Mg/Al/Fe precursors are presented in Fig. 2. It shows that they are both composed of dispersed particles and have lamellar structure with the similar average size close to

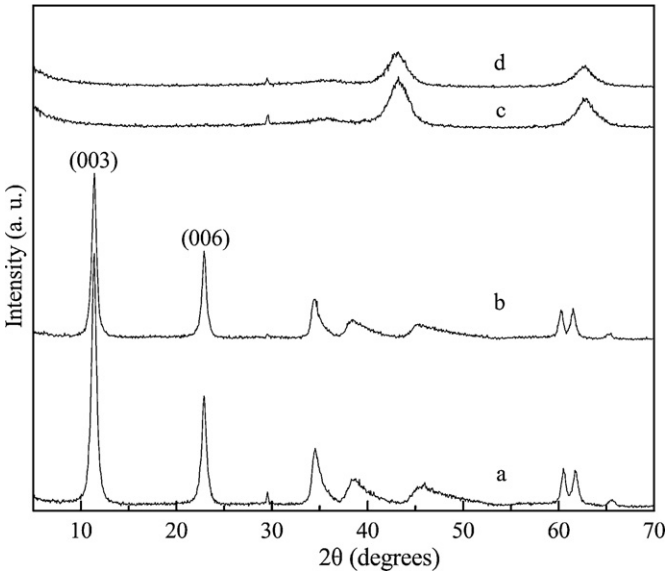

Fig. 1. The XRD patterns ((a) precursor of Mg/Al, (b) precursor of Mg/Al/Fe, (c) CH–Mg/Al, (d) CH–Mg/Al/Fe)).

50–60 nm. That is, the grain morphology and particle size practically have not changed except the better dispersion with addition of Fe^{3+}. The calcination processes only give rise to the change of lamellar structure instead of the size of particle. So CH–Mg/Al and CH–Mg/Al/Fe are also nano-sized particles.

Fig. 3 shows the pH_{PZC} of CH–Mg/Al reduced from 12.5 to 12.3 with addition of Fe^{3+} in CH–Mg/Al, which may be related to the nature property of ferric iron.

3.2. Effect of Fe^{3+} in CH–Mg/Al on adsorption properties

3.2.1. Effect of initial pH

Earlier studies have indicated that solution pH is an important parameter affecting adsorption of heavy metal ions [18,24]. The effect of pH on removal of Cr (VI) by CH–Mg/Al and CH–Mg/Al/Fe is presented in Fig. 4. It revealed that in spite of addition of Fe^{3+} in CH–Mg/Al, the amounts of Cr (VI) removed increase with the increase of pH up to a maximum then decreasing sharply and continuously for pH values higher than 3.0, and the maximum adsorption amount of CH–Mg/Al and CH–Mg/Al/Fe was 49.8 mg/g and 48.1 mg/g, respectively. However, the adsorption capacity is slightly smaller below pH 7.0 for CH–Mg/Al/Fe; while it is contrary at pH values higher than 7.0.

Chromium oxide species that can exist in aqueous solution depend on the solution pH and Cr (VI) concentration. The predominant species of Cr (VI) in solution are CrO_4^{2-}, $Cr_2O_7^{2-}$, $HCrO_4^-$, H_2CrO_4, $HCr_2O_7^{2-}$ and $Cr_3O_{10}^{2-}$. The last two ions have been tested only in solution at below pH 0 or at Cr (VI) concentration greater than 1 M. Above pH 6.8, only chromate (CrO_4^{2-}) is stable in solution, and as pH decreases into pH region 2–6, the equilibria shifts to dichromate according to the overall equilibrium [25]:

$$2CrO_4^{2-} + 2H^+ \leftrightarrow Cr_2O_7^{2-} + H_2O \quad (1)$$

Considering the properties of calcined hydrotalcites and the small influence of ferric iron on CH–Mg/Al structure from 3.1, one can say that both CH–Mg/Al and CH–Mg/Al/Fe can develop surface charges due to the structural substitutions or disorder (including defects) and reactions with ionic species in aqueous solution [26]. That is, they can form permanent and variable charges due to the adsorption of protons and hydroxide ions in solution.

In acid solution, the surfaces of CH–Mg/Al and CH–Mg/Al/Fe are protonated and therefore acquire positive charges, and the degree of protonation reduces with the increase of pH, resulting less positive charges to combine chromium from aqueous solution. But under strongly acidic conditions (below pH 3.0), a significant decline in Cr (VI) adsorption occurred, which may be caused by the dissolution of adsorbents at too low solution pH. On the other hand, although CH–Mg/Al and CH–Mg/Al/Fe have surface residual positive charges in suspension at pH values under pH_{PZC}, the hydroxide ions can react with the positive charges in alkaline solution and even occurs as deprotonation. What is more, there is competitive adsorption of hydroxide ions and chromium ions. Consequently, the Cr (VI) removal on CH–Mg/Al and CH–Mg/Al/Fe gets optimum at pH 3.0. This trend is agreement with previous studies for the removal of Cr (VI) reported by Li [18], Namasivaysam and Ranganathan [27] and Selvi [28]. The reason why the adsorption amount of CH–Mg/Al is larger than CH–Mg/Al/Fe below pH 7.0 will be discussed in the removal mechanism, but the larger adsorption amount of CH–Mg/Al/Fe above pH 7.0 remains to further research. Considering the adsorption capacity, initial pH 3.0 was used in following experiments.

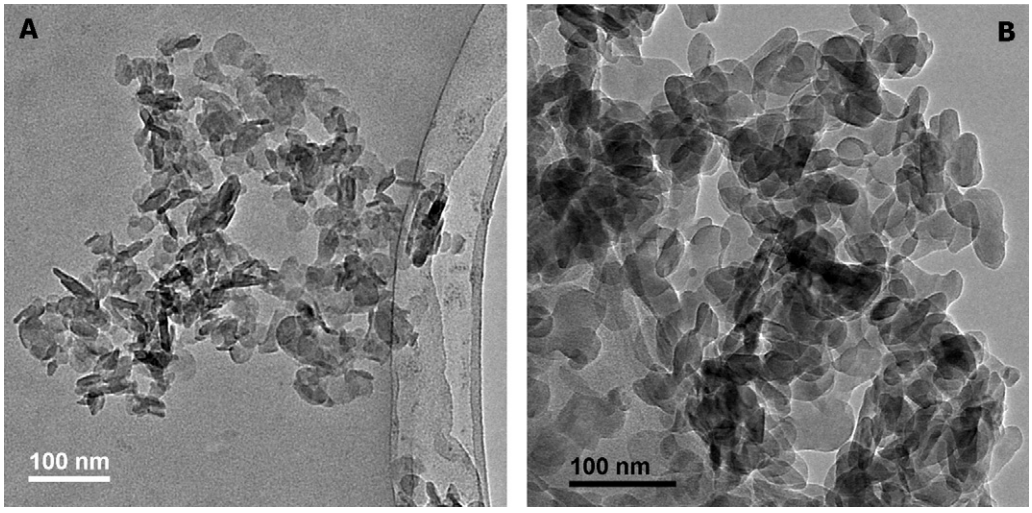

Fig. 2. TEM images of Mg/Al (A) and Mg/Al/Fe (B) precursors.

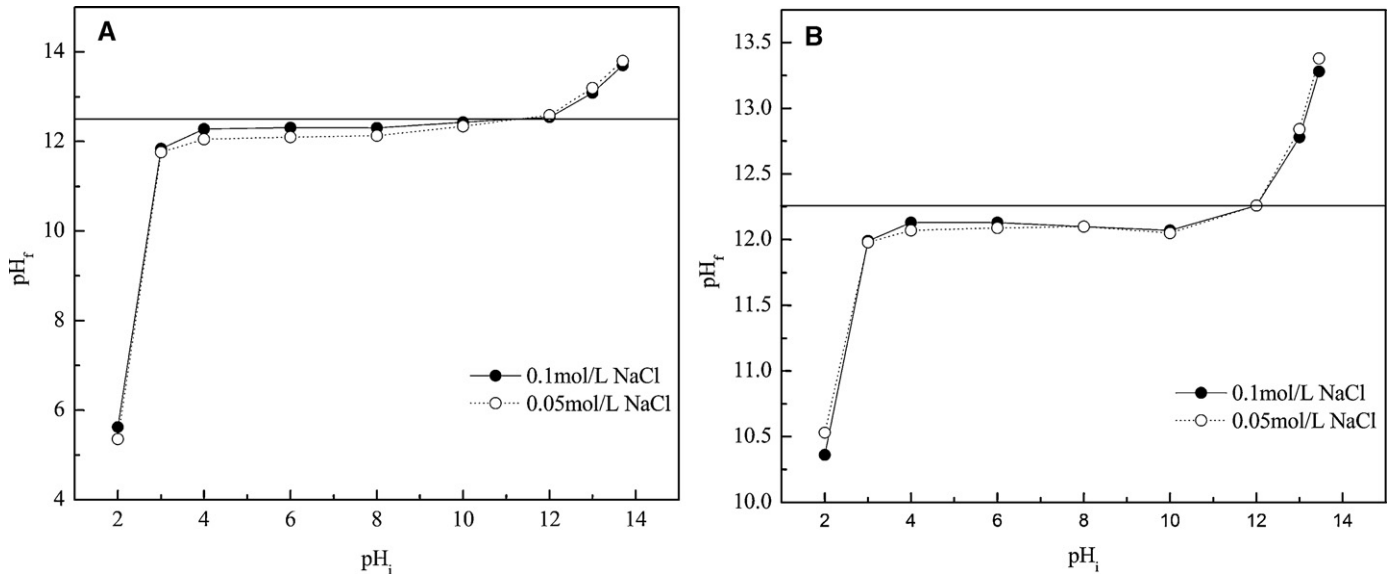

Fig. 3. The pH_{PZC} of CH–Mg/Al (A) and CH–Mg/Al/Fe (B).

3.2.2. Adsorption isotherms

Adsorption isotherms on CH–Mg/Al and CH–Mg/Al/Fe at various temperatures are shown in Fig. 5. These traces were obtained by plotting the adsorption amount versus the equilibrium concentration. It can be clearly observed that although the adsorption amounts of CH–Mg/Al and CH–Mg/Al/Fe both increase with the increase of Cr (VI) concentration and then reach saturation level when Cr (VI) concentration is beyond to a certain value (initial concentration above 110 mg/L), the maximum adsorption capacity is much smaller for CH–Mg/Al/Fe, showing the addition of Fe^{3+} in CH–Mg/Al is unfavorable to removal of Cr (VI) from aqueous solution. However, the results revealed that it was favor to removal of Cr (VI) at higher temperatures no matter whether there is ferric iron in calcined hydrotalcite.

Langmuir and Freundlich isotherms are the most commonly used models in order to describe the adsorption behavior. The two isothermal equations were expressed as:

$$\frac{C_e}{Q_e} = \frac{1}{Q_{max}K} + \frac{C_e}{Q_{max}} \quad (2)$$

$$\log \quad Q_e = \log \quad K_f + \frac{1}{n} \log \quad C_e \quad (3)$$

where C_e is the equilibrium concentration of Cr (VI) in solution (mg/L); Q_e is the amount of Cr (VI) adsorbed by the adsorbent (mg/g); Q_{max} denotes the theoretical saturated adsorption capacity of Cr (VI) (mg/g); K (L/mg) is Langmuir constant related to the adsorption–desorption energy and to the affinity of binding sites for Cr (VI) (L/mg). Both K_f (mg/g) and $1/n$ are Freundlich constants, being indicative of the extent of adsorption and the adsorption intensity, respectively. The n values between 1 and 10 represent a favorable adsorption [29].

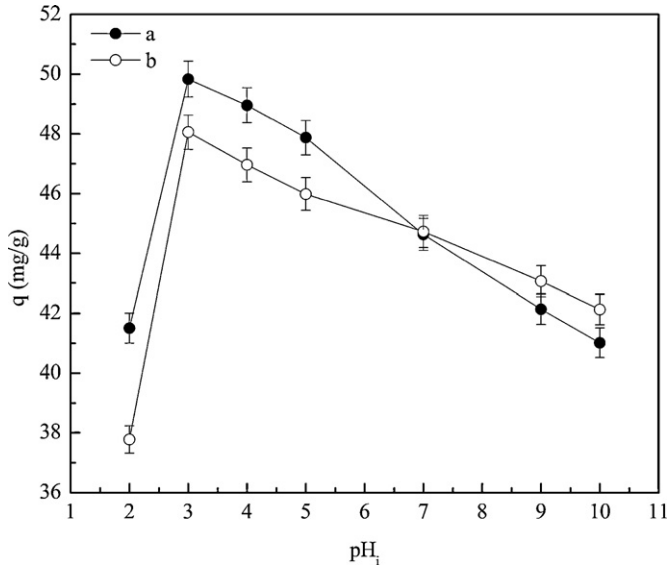

Fig. 4. Effect of initial pH: CH–Mg/Al (a) and CH–Mg/Al/Fe (b) (C_i: 50 mg/L, T: 308 K, t: 120 min).

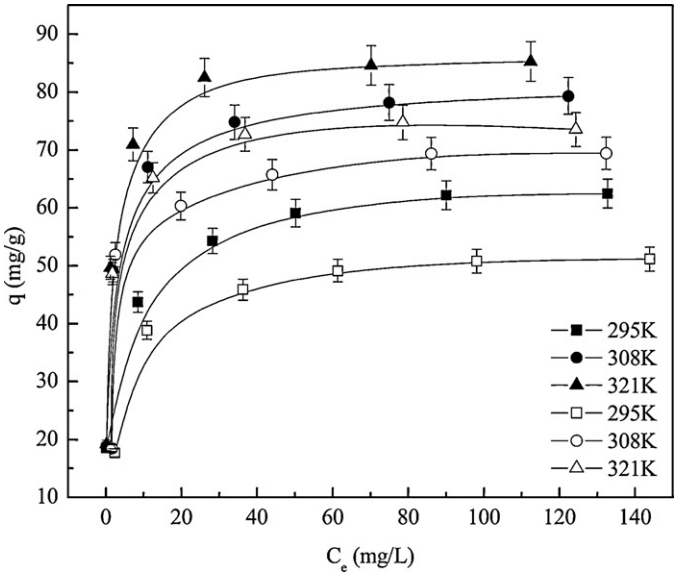

Fig. 5. Adsorption isotherms on CH–Mg/Al (the solid plots) and CH–Mg/Al/Fe (the empty plots) (pH: 3.0, t: 120 min).

Table 1
Langmuir and Freundlich isotherm parameters for adsorption of Cr (VI) on CH–Mg/Al and CH–Mg/Al/Fe.

Adsorbent	Temperature (K)	Langmuir model			Freundlich model		
		Q_{max} (mg/g)	K (L/mg)	R^2	K_f (mg/g)	n	R^2
CH–Mg/Al	295	63.6	0.339	0.999	29.3	5.9	0.987
	308	80.0	0.682	0.999	34.7	4.9	0.880
	321	85.9	0.970	0.999	36.9	4.6	0.813
CH–Mg/Al/Fe	295	52.5	0.218	0.999	17.1	4.1	0.825
	308	71.2	0.324	0.999	26.8	4.5	0.540
	321	75.4	0.484	0.999	28.9	4.4	0.559

The isotherm coefficients of CH–Mg/Al and CH–Mg/Al/Fe obtained from the slope and intercept of the linear plots were listed in Table 1. It can be seen that the adsorption fitted model has not changed with the addition of Fe^{3+} in CH–Mg/Al, they both fit better to Langmuir model based on the correlation coefficient, and the theoretical saturated adsorption capacity decreases from 63.6–85.9 mg/g to 52.5–75.4 mg/g by replacing with Fe^{3+} in CH–Mg/Al at 295–321 K. Additionally, according to Patra and colleagues [19], the Langmuir constant K can reflect the adsorption ability. He stated briefly that the larger K value indicated the greater adsorption affinity. A steady increase in K values with increasing temperature in Table 1 proves that the affinity of Cr (VI) for borh CH–Mg/Al and CH–Mg/Al/Fe increases with the rise in temperature from 295 K to 321 K, and it also indicated that it was unfavorable to Cr (VI) removal with the addition of Fe^{3+} in CH–Mg/Al. On the other hand, the K value in the present study is approximate to those previously reported by Álvarez-Ayuso and Nugteren [7] and Li et al. [18] under the same temperatures.

3.2.3. Thermodynamic parameters

With the purpose of understanding the effect of temperature on adsorption process, thermodynamic parameters should be determined by Langmuir adsorption isotherm. The thermodynamic parameters such as change in Gibbs free energy (ΔG°), enthalpy (ΔH°) and entropy (ΔS°) are calculated using the following equations:

$$\Delta G^\circ = -RT \ln K \quad (4)$$

$$\ln K = \frac{\Delta S^\circ}{R} - \frac{\Delta H^\circ}{RT} \quad (5)$$

where R is the ideal gas constant (8.314 J/mol K), T is Kelvin temperature (K) and K is Langmuir constant (L/mol). $\Delta H^\circ$and ΔS° are calculated from the slope and intercept of van't Hoff plot of $\ln K$ versus $1/T$. Thermodynamic parameter values of CH–Mg/Al and CH–Mg/Al/Fe are presented in Table 2. It can be seen that after the addition of Fe^{3+}, the average value of Gibbs free energy change (ΔG°) increased by 1.50 kJ/mol, indicating that it is disadvantageous to the spontaneous process; the enthalpy change (ΔH°) decreased by 7.86 kJ/mol, revealing that the endothermic process of adsorption needs more energy. The positive entropy changes (ΔS°) reflect the affinity of adsorbents of Cr (VI) and increase of disorderness suggesting some structural changes in adsorbate–adsorbent system [21]. It can be seen that the entropy change decreased 30.78 J/mol K by replacing with Fe^{3+}, suggesting the adsorption process tends to ordering. Therefore, although the nature of adsorption has not changed with the addition of Fe^{3+} in CH–Mg/Al, which is also spontaneous and endothermic process, the changes of thermodynamic parameter values indicated that the addition of Fe^{3+} is unfavorable to adsorption process.

Table 2
Values of thermodynamic parameters for adsorption of Cr (VI) on CH–Mg/Al and CH–Mg/Al/Fe.

Adsorbent	Temperature (K)	$\ln K_L$	ΔG° (kJ/mol)	ΔH° (kJ/mol)	ΔS° (J/mol. K)
CH–Mg/Al	295	9.78	−23.98	31.98	190.10
	308	10.48	−26.83		
	321	10.83	−28.90		
CH–Mg/Al/Fe	295	9.34	−22.90	24.12	159.32
	308	9.73	−24.92		
	321	10.13	−27.04		

3.2.4. Characterization contrast of samples before and after adsorption

The FTIR spectra of adsorbents and samples after adsorption are shown in Fig. 6. For CH–Mg/Al and CH–Mg/Al/Fe (curves a), the bands observed at around 3600–3400 cm^{-1} and the small absorp-

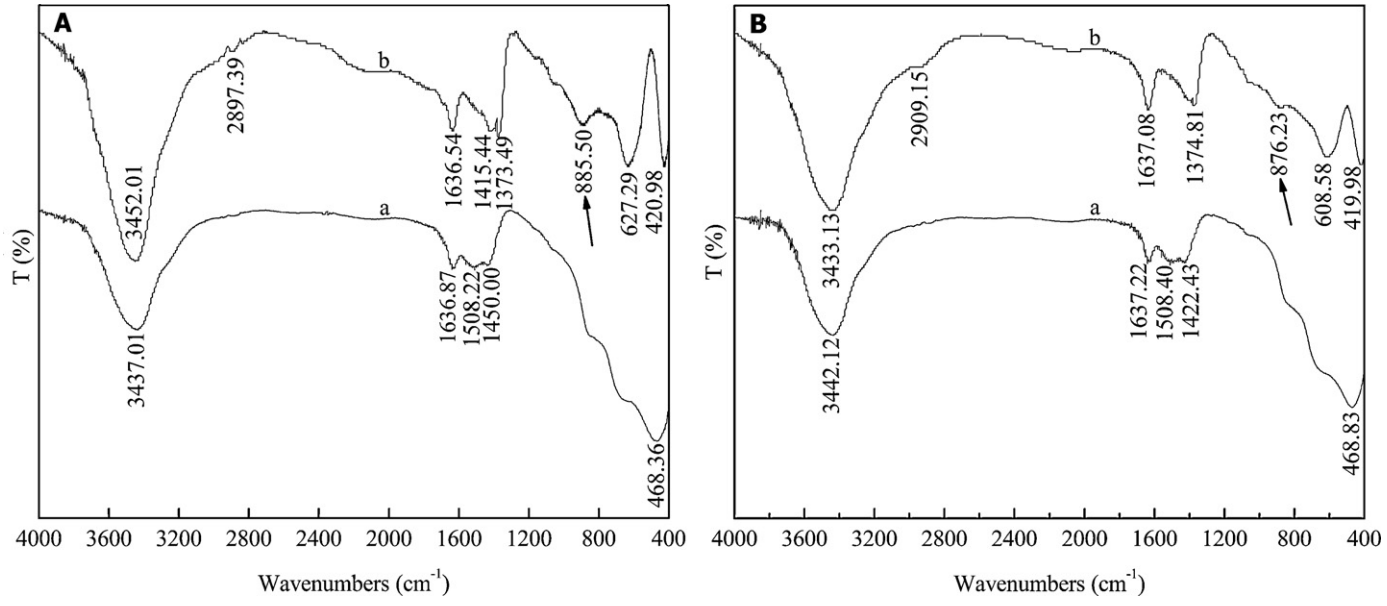

Fig. 6. FTIR spectra of adsorbents and samples after adsorption: CH–Mg/Al (A) and CH–Mg/Al/Fe (B) ((a) adsorbents; (b): samples after adsorption).

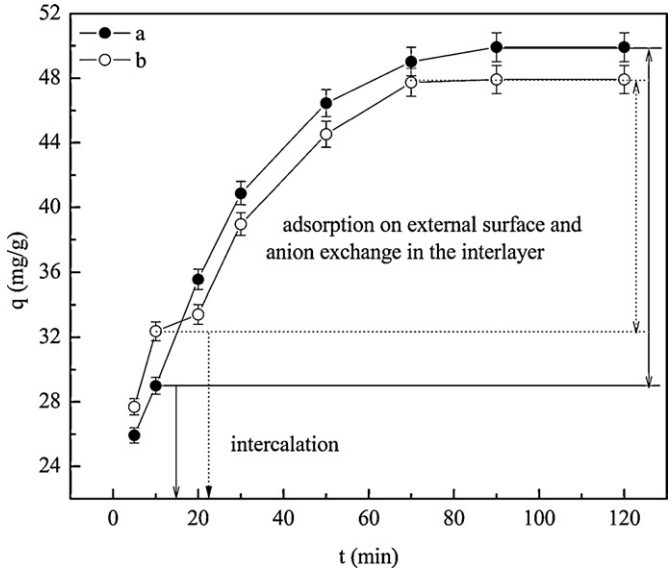

Fig. 7. Effect of contact time: CH–Mg/Al (a) and CH–Mg/Al/Fe (b) (pH: 3.0, C_i: 50 mg/L, T: 308 K).

tion peaks in the region 1700–1600 cm^{-1} are attributed to the O–H stretching vibrations and the H–O–H bending vibrations, respectively [16]. The presences of shoulders at around 1500 cm^{-1} are attributed to the disordered nature of the interlayer [30]. So there are no obvious differences by replacing with Fe^{3+} in CH–Mg/Al judging from FTIR spectra.

After adsorption (curves b), the bands at around 1500 cm^{-1} disappeared because of the reconstruction of layered structure and the carbonate–water bridging vibrations at about 2900 cm^{-1} are observed. Additionally, there are also the small absorption peaks at about 1370 cm^{-1}, which indicate the carbonate stretching vibrations (due to absorption of atmospheric CO_2 during adsorption) [6]. But there is an appearance of small absorption peak at 1415 cm^{-1} in Mg/Al/Fe ternary system compared to Mg/Al binary system. The characteristic band of free chromate appeared at 890 cm^{-1} by Nakamoto [31], but it shifted towards the lower frequency slightly for both CH–Mg/Al and CH–Mg/Al/Fe, which indicates that the Cr–O bond for Cr-adsorbent is weaker than for free chromate [18]. At the same time, the characteristic band changed from 885.50 cm^{-1} to 876.23 cm^{-1} with the existence of Fe^{3+} in CH–Mg/Al, suggesting that the binding force of Cr-adsorbent without ferric iron is stronger than that of Cr-adsorbent with ferric iron. In the spectra of both adsorbents and samples after adsorption, the bands in the vicinity of 400–800 cm^{-1} observed can be attributed to the superposition of characteristic vibrations of metal oxides.

Table 3
The interlayer space and the percentage of adsorption capacity of CH–Mg/Al and CH–Mg/Al/Fe during reconstruction process.

t (min)	d-spacing (Å)		q/q_e (%)	
	CH–Mg/Al	CH–Mg/Al/Fe	CH–Mg/Al	CH–Mg/Al/Fe
Precursors	7.78	7.74		
10	7.55	7.66	58.1	67.5
30	7.66	7.66	81.9	81.3
90	7.70	7.71	100	100
120	7.75	7.79	100	100

3.3. *Effect of Fe^{3+} in CH–Mg/Al on removal mechanism*

The influence of contact time on removal of Cr (VI) was shown in Fig. 7. It revealed that the amounts of adsorbed Cr (VI) increased with contact time and then attained the "plateau" at contact time of 90 min and 70 min for CH–Mg/Al and CH–Mg/Al/Fe, respectively, which indicated that the existence of Fe^{3+} in CH–Mg/Al makes the Cr (VI) removal faster. And the adsorption capacity of CH–Mg/Al/Fe is slightly larger than CH–Mg/Al within 10 min, while it is contrary within the remaining time.

In order better to understand the removal mechanism, the XRD patters of four samples at 10 min, 30 min, 90 min and 120 min during adsorption process for each adsorbent were shown in Fig. 8. It indicated that CH–Mg/Al and CH–Mg/Al/Fe both recovered their original structure within 10 min, showing the regeneration process was fast and efficient. At the same time, it can be seen that the characteristic peaks of hydrotalcites at (0 0 3) and (0 0 6) slightly shifted to lower degrees after 90 min for CH–Mg/Al and CH–Mg/Al/Fe. The interlayer space and the percentage of adsorption capacity on CH–Mg/Al and CH–Mg/Al/Fe during reconstruction process are presented in Table 3. It revealed that the interlayer space gradually

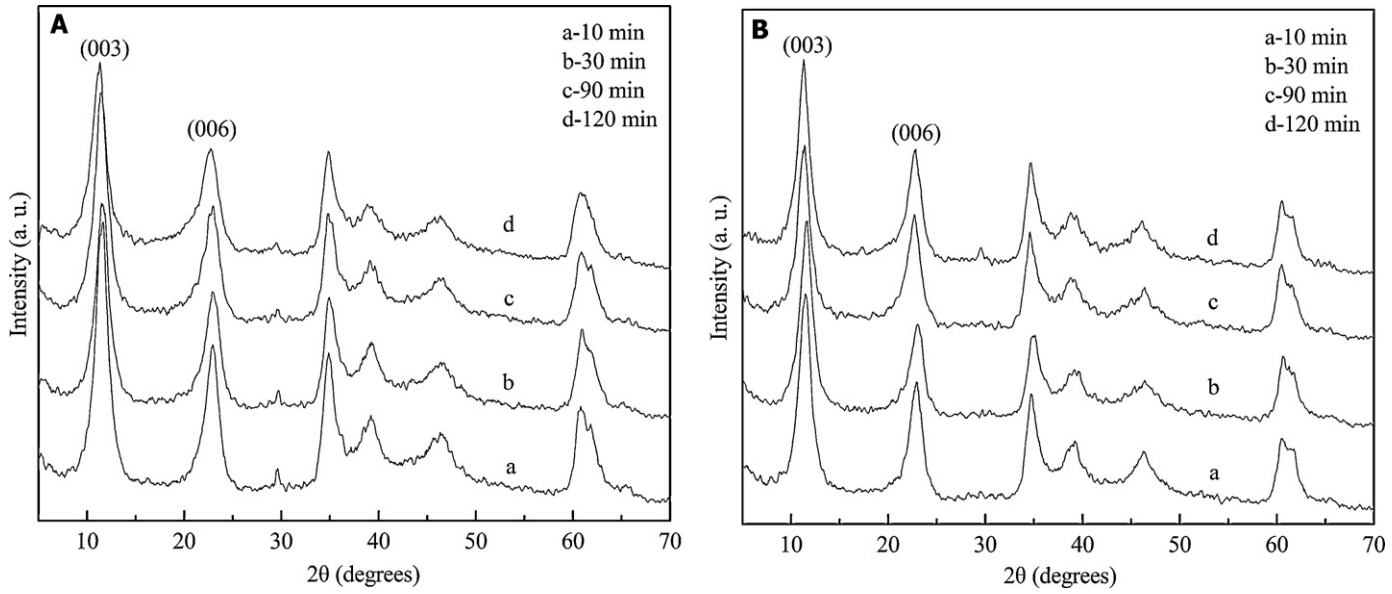

Fig. 8. The XRD patterns of CH–Mg/Al (A) and CH–Mg/Al/Fe (B) at different contact times during reconstruction process.

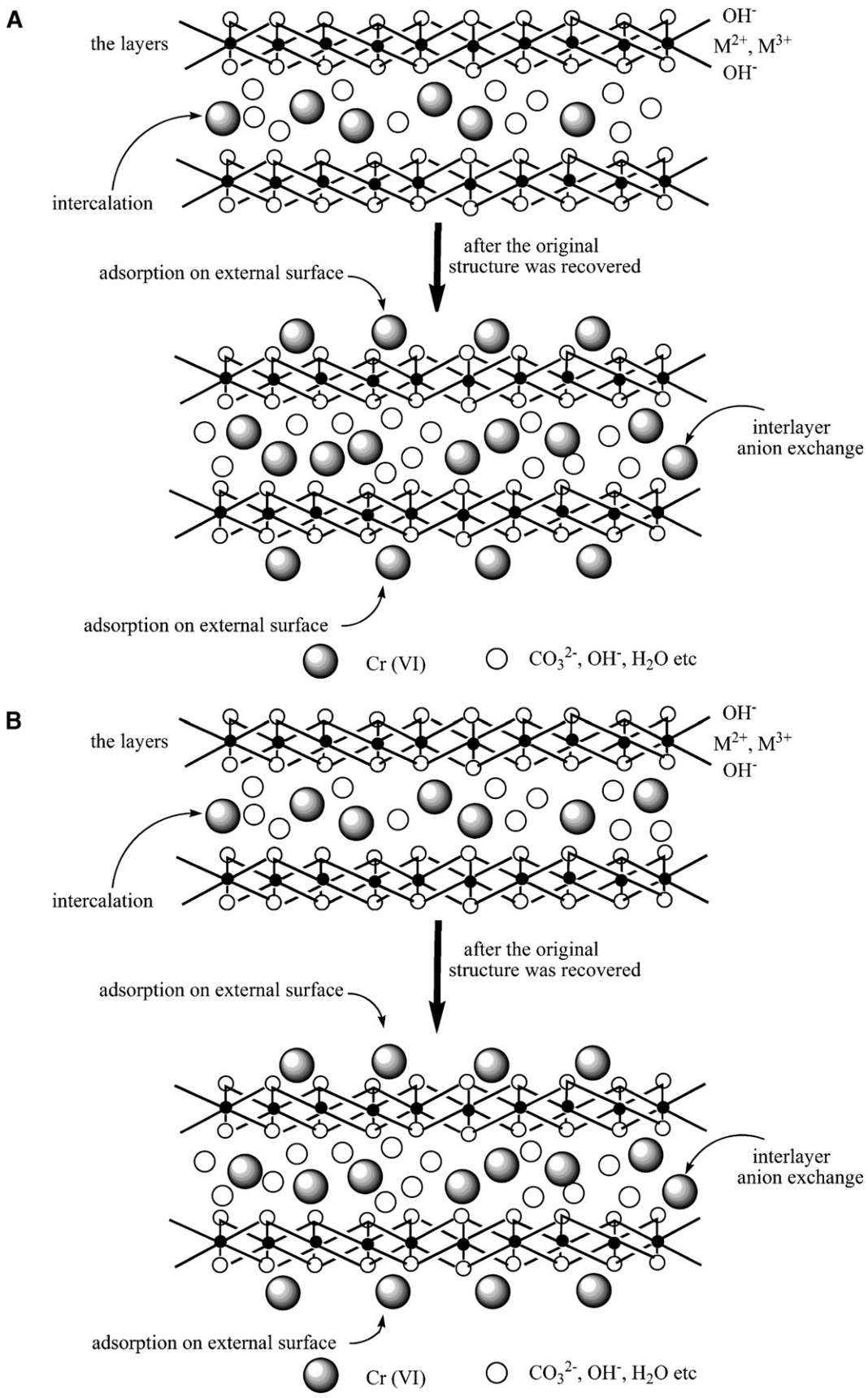

Fig. 9. The removal mechanism of Cr (VI) on CH–Mg/Al (A) and CH–Mg/Al/Fe (B).

increases within the whole adsorption process. This may be related to the fact that d-spacing of hydrotalcites gradually decreases during the thermal decomposition because of the elimination of water molecules and carbonate anions in the interlayer step by step. Compared to their precursors, there are no significant changes in the interlayer space after adsorption equilibrium; this may be resulted from the flat orientation of chromium in the interlayer [32]. Meanwhile, the average d-spacing values of CH–Mg/Al and CH–Mg/Al/Fe after adsorption equilibrium are both characteristic of carbonate anions due to their strongest capacities to stabilize hydrotalcite structure, and the carbonates in the interlayer can be regarded as the absorption of atmospheric CO_2 [33]. However, the average value of CH–Mg/Al/Fe is larger than CH–Mg/Al. The different interlayer space of the same anion perhaps is due to the difference of solution pH caused by different hydrolysis degree of metal oxides during the regeneration process.

Although CH–Mg/Al and CH–Mg/Al/Fe both recover their original structure within 10 min, the adsorption amounts do not reach saturation level in this period seen from the adsorption percentage. That is, the mechanism of Cr (VI) removal involved not only intercalation but adsorption on external surface of the layers or interlayer anion exchange. At the same time, Table 3 showed that the proportion of intercalation of CH–Mg/Al increased from 58.1% to 67.5% with the addition of Fe^{3+}, revealing the replacing with Fe^{3+} is advantage to the removal of Cr (VI) within intercalation, but the overall adsorption amount of CH–Mg/Al/Fe is also smaller than CH–Mg/Al. This may be related to the different mechanism after the layered structure was recovered. When the original structure was recovered from aqueous solution, the anion removal on hydrotalcites refers to two different mechanisms: (i) adsorption on external surface (faster) and (ii) interlayer ion exchange (slower) [1,23]. And generally, the adsorption process is faster than ion exchange because of the strong interaction between negative ions and the positive external surface and due to the high exposition of the external surface of the hydrotalcites, while ion exchange is a diffusion process [23]. On the other hand, Triantafyllidis et al. [34] indicated that the replacement of Al^{3+} by Fe^{3+} in layered double hydroxide strengthens the bond between double-hydroxide layers and carbonates in the interlayer by increasing the positive surface charge. Bruna et al. [20] also stated that the presence of Fe^{3+} in hydrotalcite would increase the attraction of anions in the interlayer by layers due to the greater polarizing power of Fe^{3+} than Al^{3+} and makes its displacement more difficult. Therefore, we propose the phenomenon that the adsorption of CH–Mg/Al/Fe reached equilibrium more quickly and the adsorption capacity was smaller than CH–Mg/Al is due to the nature property of ferric iron, which makes the interlayer anion exchange more difficult, following after the reconstruction of the structure. The detailed mechanism of Cr (VI) removal on CH–Mg/Al and CH–Mg/Al/Fe is described in Fig. 9.

4. Conclusions

CH–Mg/Al and CH–Mg/Al/Fe were prepared and characterized in this study. The influence of Fe^{3+} in CH–Mg/Al on removal of Cr (VI) from aqueous solution was studied from aspects of structure characteristics, adsorption properties and the removal mechanism. The results are summarized as follows:

(1) The XRD patters, TEM images and FTIR spectra showed that replacing Al^{3+} with Fe^{3+} has almost not changed the structure of CH–Mg/Al. Mg/Al and Mg/Al/Fe precursors are both nano-sized particles with lamellar structure. The only difference is the lower intensities, the smaller interlayer space and the better dispersion for Mg/Al/Fe precursor. The pH_{PZC} reduced from 12.5 to 12.3 with addition of Fe^{3+}.

(2) The removal of Cr (VI) gets the maximum at pH 3.0 for both CH–Mg/Al and CH–Mg/Al/Fe. The isotherms indicated that the adsorption both fitted better to Langmuir model, but the theoretical saturated adsorption capacity reduces from 63.6–85.9 mg/g to 52.5–75.4 mg/g by replacing with Fe^{3+} at 295–321 K, suggesting that the existence of Fe^{3+} in CH–Mg/Al is unfavorable to Cr (VI) removal. Additionally, although thermodynamic parameter values revealed the adsorption natures on CH–Mg/Al and CH–Mg/Al/Fe are endothermic and spontaneous processes, the value changes indicated the addition of Fe^{3+} in CH–Mg/Al goes against the adsorption process.

(3) The reconstruction processes of CH–Mg/Al and CH–Mg/Al/Fe were fast and efficient, but the adsorption on CH–Mg/Al/Fe reached equilibrium faster. The results showed that removal mechanism involved not only intercalation but also adsorption on external surface of the layers and interlayer anion exchange for both CH–Mg/Al and CH–Mg/Al/Fe. Furthermore, it also indicated that intercalation accounts for a large proportion during the removal process whatever for CH–Mg/Al, or for CH–Mg/Al/Fe. Additionally, the replacement of Al^{3+} by Fe^{3+} in hydrotalcite led to the interlayer anion exchange more difficult.

References

[1] F. Cavani, F. Trifiro, A. Vaccari, Hydrotalcite-type anionic clays: preparation, properties and applications, Catal. Today 11 (1991) 173–301.
[2] W.T. Reichle, Catalytic reactions by thermally activated, synthetic, anionic clay minerals, J. Catal. 94 (1985) 547–557.
[3] S. Mandal, S. Mayadevi, Adsorption of fluoride ions by Zn–Al layered double hydroxides, Appl. Clay Sci. 40 (2008) 54–62.
[4] L. Yang, Z. Shahrivari, P.K.T. Liu, Removal of trace levels of arsenic and selenium from aqueous solutions by calcined and uncalcined layered double hydroxides (LDH), Ind. Eng. Chem. Res. 44 (2005) 6804–6815.
[5] M. Shigeo, Physico-chemical properties of synthetic hydrotalcites in relation to composition, Clay. Clay Miner. 28 (1980) 50–56.
[6] E. Ramos-Ramírez, N.L. Gutiérrez Ortega, C.A. Contreras Soto, M.T. Olguín Gutiérrez, Adsorption isotherm studies of chromium (VI) from aqueous solution using sol–gel hydrotalcite-like compounds, J. Hazard. Mater. 172 (2009) 1527–1531.
[7] E. Álvarez-Ayuso, H.W. Nugteren, Purification of chromium (VI) finishing wastewaters using calcined and uncalcined Mg–Al–CO_3-hydrotalcite, Water Res. 39 (2005) 2535–2542.
[8] E. Álvarez-Ayuso, A. García-Sánchez, X. Querol, Adsorption of Cr (VI) from synthetic solution and electroplating wastewaters on amorphous aluminium oxide, J. Hazard. Mater. 142 (2007) 191–198.
[9] L.S. Wei, G. Yang, R. Wang, W. Ma, Selective adsorption and separation of chromium (VI) on the magnetic iron–nickel oxide from waste nickel liquid, J. Hazard. Mater. 164 (2009) 1159–1163.
[10] R.S. Juang, R.C. Shiau, Metal removal from aqueous solutions using chitosan-enhanced membrane filtration, J. Membr. Sci. 165 (2000) 159–167.
[11] S.S. Baral, S.N. Das, P. Rath, G.R. Chaudhury, Chromium (VI) removal by calcined bauxite, Biochem. Eng. J. 34 (2007) 69–75.
[12] W.S. Wan Ngah, M.A.K.M. Hanafiah, Removal of heavy metal ions from wastewater by chemically modified plant wastes as adsorbents: a review, Bioresour. Technol. 99 (2008) 3935–3948.
[13] V.K. Gupta, A. Rastogi, A. Nayak, Adsorption studies on the removal of hexavalent chromium from aqueous solution using a low cost fertilizer industry waste material, J. Colloid Interface Sci. 342 (2010) 135–141.
[14] S. Babel, T.A. Kurniawan, Cr (VI) removal from synthetic wastewater using coconut shell charcoal and commerical activated carbon modified with oxidizing agents and/or chitosan, Chemosphere 54 (2004) 951–967.
[15] M. Dakily, M. Khamis, A. Manassra, M. Mer'eb, Selective adsorption of chromium (VI) in industrial wastewater using low-cost abundantly available adsorbents, Adv. Environ. Res. 6 (2002) 533–540.
[16] S. Mor, K. Ravindra, N.R. Bishnoi, Adsorption of chromium from aqueous solution by activated alumina and activated charcoal, Bioresour. Technol. 98 (2007) 954–957.
[17] N.K. Lazaridis, D.D. Asouhidou, Kinetics of sorptive removal of chromium (VI) from aqueous solutions by calcined Mg–Al–CO_3 hydrotalcite, Water Res. 37 (2003) 2875–2882.
[18] Y. Li, B. Gao, T. Wu, D. Sun, X. Li, B. Wang, F. Lu, Hexavalent chromium removal from aqueous solution by adsorption on aluminum magnesium mixed hydroxide, Water Res. 43 (2009) 3067–3075.
[19] J. Das, B.S. Patra, N. Baliarsingh, K.M. Parida, Calcined Mg–Fe–CO_3 LDH as an adsorbent for the removal of selenite, J. Colloid Interface Sci. 316 (2007) 216–223.
[20] F. Bruna, R. Celis, I. Pavlovic, C. Barriga, J. Cornejo, M.A. Ulibarri, Layered double hydroxides as adsorbents and carriers of theherbicide (4-chloro-2-

methylphenoxy) acetic acid (MCPA): systems Mg–Al, Mg–Fe and Mg–Al–Fe, J. Hazard. Mater. 168 (2009) 1476–1481.
[21] J. Das, D. Das, G.P. Dash, D. Das, K. Parida, Studies on Mg/Fe hydrotalcite-like compound: removal of chromium (VI) from aqueous solution, Int. J. Environ. Stud. 61 (2004) 605–616.
[22] L.Y. Tian, W. Ma, M. Han, Adsorption behavior of Li^+ onto nano-lithium ion sieve from hybrid magnesium/lithium manganese oxide, Chem. Eng. J. 156 (2010) 134–140.
[23] O.P. Ferreira, S.G. de Moraes, N. Durán, L. Cornejo, O.L. Alves, Evaluation of boron removal from water by hydrotalcite-like compounds, Chemosphere 62 (2006) 80–88.
[24] V.K. Gupta, A.K. Shrivastava, N. Jain, Biosorption of chromium from aqueous solution by green algae spirogyra species, Water Res. 35 (2001) 4079–4085.
[25] B.M. Weckhuysen, I.E. Wachs, R.A. Schoonheydt, Surface chemistry and spectroscopy of chromium in inorganic oxides, Chem. Rev. 96 (1996) 3327–3349.
[26] W. Stumm, Chemistry of the solid–water interface, in: Werner Stumm Surface Charge and the Electric Double Layer, Wiley, John & Sons, Inc., New York, 1992, pp. 43–86.
[27] C. Namasivaysam, K. Ranganathan, Waste Fe (III)/Cr (III) hydroxide as adsorbent for the removal of Cr (VI) from aqueous solution and chromium plating industry wastewater, Environ. Pollut. 82 (1993) 255–261.
[28] K. Selvi, S. Pattabhi, K. Kadirvelu, Removal of Cr (VI) from aqueous solution by adsorption onto activated carbon, Bioresour. Technol. 80 (2001) 87–89.
[29] S. Chatterjee, D.S. Lee, M.W. Lee, S.H. Woo, Enhanced adsorption of congo red from aqueous solutions by chitosan hydrogel beads impregnated with cetyl trimethyl ammonium bromide, Bioresour. Technol. 100 (2009) 2803–2809.
[30] M.J. Hernandez-Moreno, M.A. Ulibarri, J.L. Rendon, C.J. Serna, IR Characteristics of hydrotalcite-like compounds, Phys. Chem. Miner. 12 (1985) 34–38.
[31] K. Nakamoto, Infrared and Raman of Inorganic and Coordination Compounds, fifth ed., John Wiley & Sons Inc., New York, 1986.
[32] L.P. Cardoso, J.B. Valim, Study of acids herbicides removal by calcined Mg–Al–CO_3-LDH, J. Phys. Chem. Solids 67 (2006) 987–993.
[33] S. Miyata, Anion-exchange properties of hydrotalcite-like compounds, Clay. Clay Miner. 31 (1983) 305–311.
[34] K.S. Triantafyllidis, E.N. Peleka, V.G. Komvokis, P.P. Mavros, Iron-modified hydrotalcite-like materials as highly efficient phosphate sorbents, J. Colloid Interface Sci. 342 (2010) 427–436.